NASA TECHNICAL NOTE

NASA TN D-2747

NASA TN D-2747

FACILITY FORM 602

N65-20879
(ACCESSION NUMBER)

23
(PAGES)

(NASA CR OR TMX OR AD NUMBER)

(THRU)
1
(CODE)
30
(CATEGORY)

A METEOROID ENVIRONMENT FOR NEAR-EARTH, CISLUNAR, AND NEAR-LUNAR OPERATIONS

by Paige B. Burbank, Burton G. Cour-Palais, and William E. McAllum

Manned Spacecraft Center
Houston, Texas

GPO PRICE $ ______

~~OTS~~ CFSTI PRICE(S) $ 1.00

Hard copy (HC) ______

Microfiche (MF) $0.50

NATIONAL AERONAUTICS AND SPACE ADMINISTRATION • WASHINGTON, D. C. • APRIL 1965

NASA TN D-2747

A METEOROID ENVIRONMENT FOR NEAR-EARTH, CISLUNAR, AND NEAR-LUNAR OPERATIONS

By Paige B. Burbank, Burton G. Cour-Palais,
and William E. McAllum

Manned Spacecraft Center
Houston, Texas

NATIONAL AERONAUTICS AND SPACE ADMINISTRATION

For sale by the Clearinghouse for Federal Scientific and Technical Information
Springfield, Virginia 22151 – Price $1.00

A METEOROID ENVIRONMENT FOR NEAR-EARTH,

CISLUNAR, AND NEAR-LUNAR OPERATIONS

By Paige B. Burbank, Burton G. Cour-Palais, and William E. McAllum
Manned Spacecraft Center

SUMMARY

20879

A meteoroid environment model is presented for operations in the near-earth and cislunar regions and on the lunar surface. The model includes the average logarithmic flux-mass relationship, velocity, and mass density for sporadic, stream, and secondary (lunar surface ejecta) meteoroids. An annual variation of the average sporadic flux and the time-dependent variation of the stream to the sporadic flux ratio for 18 streams is graphically represented. The variation of the stream flux with mass is considered, and orbital elements are provided for the major streams.

Author I

INTRODUCTION

One of the principal parameters to be considered in the design of space vehicles is the hazard imposed by extraterrestrial debris. The impingement of high-velocity particles on thin-skinned pressurized structures can result in minute punctures and gradual depressurization of the space vehicle or catastrophic ruptures by explosive decompression. Interaction of the vaporized skin, caused by absorption of the kinetic energy of the impinging particle, with the space-vehicle atmosphere can result in oxidative explosions with resultant high-temperature and pressure fluctuations. Impingement of high-velocity particles can also result in failure of various spacecraft components or failure of the heat shield during reentry because of puncture. The hazard includes damage by erosion to extremely thin surfaces, solar panels, viewing ports, and optical systems.

The purpose of this paper is to furnish design criteria for the meteoroid environment of the earth-moon system and is not meant to be a treatise on meteoroid technology nor a compilation of papers related to meteoroid criteria. This meteoroid environment is the result of the development of several trial model environments that have been assessed and modified by spacecraft manufacturers, scientists, and engineers associated with space environment and spacecraft hardware.

The scope includes the physical and dynamic characteristics of individual particles in space and the flux of both sporadic and stream meteoroids. The

environment is applicable to interplanetary space near the earth (at an altitude of $\geq$ 70 km) and in the cislunar and lunar (to the surface of the moon) regions. The density and orbit (velocity) is defined for a range of meteoroid sizes from a minimum defined by the Poynting-Robertson effect (ref. 1) to a maximum of 1 gram.

The continued work in the many aspects of space environment will require a continued updating of these criteria to include the most recent and accurate data.

SYMBOLS

a	semimajor axis, astronomical units (A.U.)
F	ratio of accumulative meteoroid stream flux to the sporadic meteoroid flux
H	altitude above surface of the shielding body (see sketch A)
M_v	visual magnitude
m	mass, grams
N	flux, particles/unit area - unit time (units of area and time are defined with each equation)
p	point of perihelion
q	perihelion distance, A.U.
R	radius of shielding body
S	sun
V	velocity, km/sec
V_s	velocity of stream, km/sec
Υ	heliocentric position of the vernal equinox, deg
ϵ	eccentricity
ζ	shielding factor
θ	$\frac{1}{2}$ the angle subtended by the shielding body
ι	inclination of meteoroid orbital plane

π	$\Omega + \omega$, longitude of perihelion, deg
ρ	density, gm/cm^3
Ω	longitude of ascending node, deg
$\bar{\Omega}$	ascending node
$\underline{\mho}$	descending node
ω	latitude of perihelion

Subscripts:

0, n	meteor visual magnitude

TERMINOLOGY

In this paper the word "meteoroid" is used as a general term referring to particles traveling in space. A "meteor" is the visual, photographic, or electromagnetic phenomenon associated with the interaction of a meteoroid with the earth's atmosphere. A "meteorite" is that portion of a meteoroid that has survived the interaction with the earth's atmosphere and is found on the surface of the earth. "Micrometeorite" is a qualitative term for meteorites that have a large surface area to mass ratio, and the energy of interaction with the earth's atmosphere is radiated without large physical changes. "Sporadic" meteoroids are individual particles having random orientation and no known relation to any other particle. "Stream" meteoroids consist of particles in relatively close proximity, each particle having a similar, but independent, orbit about the sun.

GENERAL REMARKS ON SPACE DEBRIS

The presence of space debris within the solar system is indicated by the following:

(1) The solar Fraunhofer-corona and zodiacal light are caused by the reflection and refraction of sunlight by particles ranging in size from about 0.2 micron to 300 microns in diameter that are located between the earth and the sun. A similar phenomenon denoted as gegenschein emanates from particles at distances greater than 1 A.U.

(2) Ground-based observations of meteors.

(3) The recovery of meteorites from many different areas on the earth's surface and micrometeorites from the polar regions.

(4) The initial results obtained with particle-flux sensors on rocket probes and earth satellites at altitudes greater than 100 km.

In size, the debris ranges from the body that caused the largest meteorite crater found on the earth, the 2-mile-diameter Ungava crater in Quebec, to the particle limited by solar pressure and the Poynting-Robertson effect. The Poynting-Robertson effect, as defined in reference 1, is the drag caused by the reemission and reflection of incident solar radiation. Radiation emitted by the particle in the direction of motion has a slightly higher frequency, and therefore higher energy, than the radiation emitted in the opposite direction. The resultant radiation pressure differential decelerates the particle. As an example, the Poynting-Robertson effect would cause a 500-micron-diameter particle located in Halley's comet and having a density of 4 gm/cm^3 to spiral into the sun in 10^7 years. Solar radiation pressure imposes a lower limit on the Poynting-Robertson effect, and all particles smaller than the limit are swept out of the solar system. The limiting diameter is presented (ref. 2) as 0.3 micron for a metallic particle and 0.2 micron for a dielectric particle. In reference 3, the smallest particle diameter required to produce the zodiacal light is given as 0.16 micron and 4.1 microns for the metallic and the dielectric particles, respectively. The existence of particles smaller than the radiation pressure limit is explained by a continuous creation by the disintegration of the larger "fluffy" particles (ref. 4).

There are at least five hypothesized sources of space debris: (1) cometary ejection or disintegration, which probably contributes more than 90 percent of the total space debris; (2) grinding and fragmentation of asteroids, which contribute between 2 and 10 percent of the total; (3) ejected material from the surface of the moon; (4) interstellar capture, which probably contributes about 1 percent of the total; and (5) condensation of interplanetary gas.

Meteoroid Composition

The source of space debris gives an indication of the meteoroid density. Asteroids are believed to vary from 3 to 9 gm/cm^3. The chemical analysis of meteorites implies the composition of asteroidal meteoroids. The meteorites have been categorized in the following table from reference 5.

CLASSIFIED METEORITE FALLS

[Prior's Catalogue 1953]

Class	Number	Percent
Irons	42	6.6
Stoney-Irons	12	1.9
Chondrites	523	82.8
Achondrites	56	8.7

Additional definition of micrometeorite composition has been obtained with the "Venus Fly Trap" (ref. 4). A survey of 17.8 mm^2 of the "Fly Trap" sampling area indicated 133 particles varying in size from 0.1 to 1 micron. Eleven particles greater than 1 micron in diameter were found by extending the surveyed sampling area to 18.5 mm^2. Although electron microscope diffraction patterns of some particles indicate compositions of nickel monoxide and taenite, reference 4 classifies the particles in the three broad terms: fluffy, medium, and high density.

Whipple, in reference 6, states that the majority (greater than 90 percent) of meteors are of cometary origin and has defined the comet composition as an icy conglomerate of mineral particles. The low density, high porosity, and frangibility of meteoroids are also indicated by flaring meteors (those having varying luminosity). As discussed in reference 7, a dynamic pressure of $\frac{1}{50}$ of an atmosphere will cause a meteoroid to shatter. The conglomerate structure and related low-bulk density will have a minimum particle size that can include voids. For smaller sizes, the bulk density will increase to the density of mixtures of the heavier elements (in some comets, nickel and iron) that have been identified by spectral emissions of comets.

In reference 8, a single meteoroid density is used throughout the mass range. The density of 0.44 gm/cm^3 was obtained by simultaneous solution of luminosity and drag equations for several meteors.

Meteoroid Velocity

The geocentric velocity of the primary particle flux can vary from 11 km/sec to 72 km/sec. The lower limit corresponds to the gravitational potential of the earth; the upper limit is the summation of the earth's orbiting velocity plus the parabolic velocity at 1 A.U., in the solar system, of a retrograde particle in the ecliptic plane. The radar measurement of the velocity of 11 073 meteors (ref. 9) by McKinley of the National Research Council of Canada, as shown in figure 1, indicates that very few meteors have hyperbolic trajectories and hence geocentric velocities > 72 km/sec. Those that do have hyperbolic trajectories could have been changed by planetary attraction. The data of figure 1 are for meteors with a $M_v \approx 6$ and less; the average

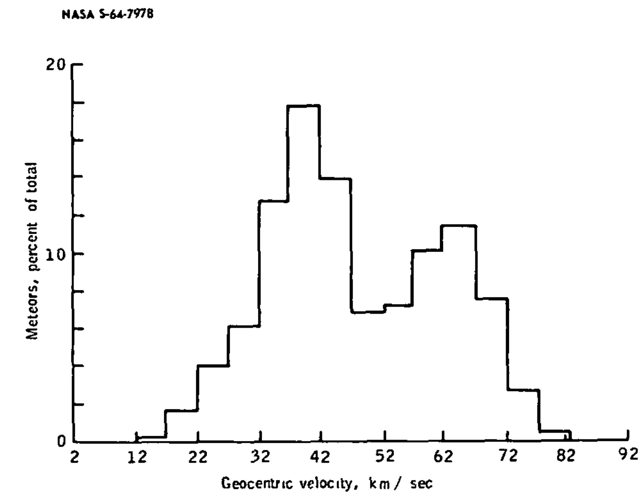

Figure 1. - Velocity distribution of 11,073 meteors with $M_v \approx 6$ or less.

velocity for a constant mass cannot be obtained from this figure. The meteor intensity (ion density) increases with velocity and results in an increased detection of smaller meteors. The measuring system does not detect the increased number of these small meteors having a lower velocity. The velocity variation with visual magnitude as presented in reference 10 assumes a geocentric velocity of 28 km/sec for meteors in the range of visual magnitude of 0 to 7. The increasing influence of radiation pressure with decreasing particle size is taken into consideration by reducing the velocity 1 km/sec per visual magnitude to a constant value of 15 km/sec at a visual magnitude of 20; 15 km/sec is assumed constant for all larger visual magnitudes. In reference 8, a mean velocity of 22 km/sec is used.

Meteoroid Streams

Noticeable increases in the average hourly rate of meteor activity occur at regular intervals during the calendar year. These increases are caused by the earth's passage through a stream of particles traveling in similar heliocentric orbits and generally assumed to be cometary debris. The orbital elements, periods of occurrence, and ratio of maximum accumulative meteoroid stream flux to the sporadic meteoroid flux of 18 of the more prominent streams, as determined from references 11 to 13, are listed in table I and figure 2.

Figure 3 illustrates the orbital paths of some of these streams projected on the ecliptic plane at 1 A.U.

NASA-S-64 7973

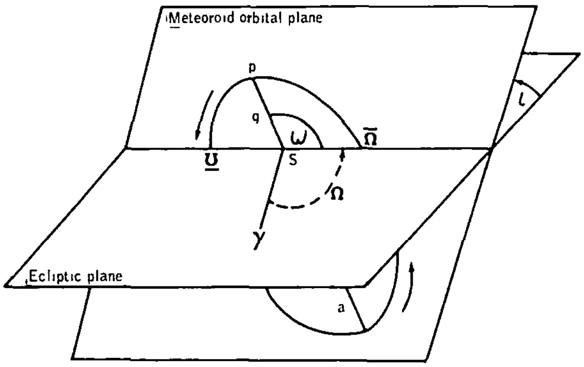

a = semi-major axis, A.U.

p = point of perihelion

q = perihelion distance, A.U.

S = sun

γ = heliocentric position of the vernal equinox, deg

i = inclination of meteoroid orbital plane, deg

$\pi = \Omega + \omega$

Ω = longitude of ascending node, deg

$\overline{\Omega}$ = ascending node

$\underline{\mho}$ = descending node

ω = latitude of perihelion, deg

Figure 2. - Orbital elements for major meteoroid streams.

NASA S-64-7977

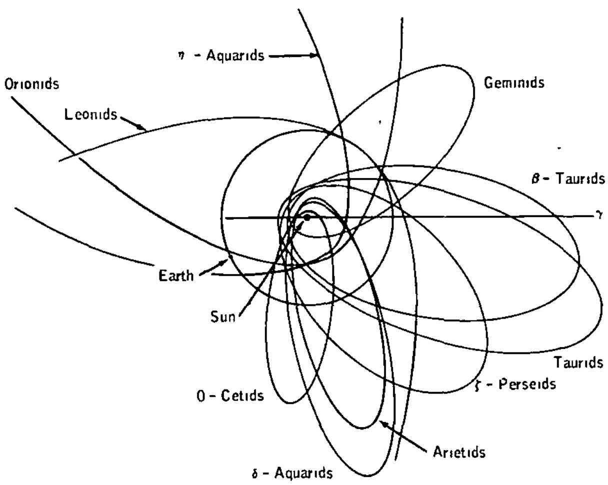

Figure 3. - Orbits of meteoroid streams intersecting the ecliptic plane.

TABLE I.- ORBITAL ELEMENTS FOR MAJOR METEOROID STREAMS

[Orbital elements defined in fig 2]

Name	Period of activity	Date of maximum	F_{max} (a)	Ω, deg	π, deg	ω, deg	ι, deg	ε	q, A U.	a, A U.	Velocity: Geocentric, km/sec	Velocity: Heliocentric, km/sec	Period, years
Quadrantids[b]	Jan. 2 to 4	Jan. 3	8.0	282	92	166	67	0 46	0.97	1 7	42	39	13
Lyrids	Apr. 19 to 22	Apr. 21	85	30 5	--	210	81	88	.90	--	48	40	19 8
η-Aquarids	May 1 to 8	May 4 to 6	2.2	45	152	108	162	.96	.66	17 95	64	41	11
O-Cetids	May 14 to 23	May 14 to 23	2.0	238	89	211	34	.91	.11	1.3	37	33	1.5
Arietids	May 29 to June 19	June 6	4.5	77	106	29	21	.94	.09	1 6	38	34	1 8
ζ-Perseids	June 1 to 16	June 6	3.0	78	--	59	4±2	.79	35	1.6	29	35	2.2
β-Taurids	June 24 to July 5	June 28	2.0	276	162±4	246±4	9±4	.86	.36	2.5	31	37	3.3
δ-Aquarids	July 26 to Aug 5	July 28	1.5	305	101±2	156±2	24±5	.96	08	1 8	40	35	3 6
Perseids	July 15 to Aug. 18	Aug. 10 to 14	5.0	142	--	155	114	.96	.97	23	60	42	109.5
Giacobinids[b]	Oct 9 to 10	Oct. 10	20	196	--	172	30 8	.72	99	3.5	23	41	6.57
Orionids	Oct. 15 to 25	Oct 20 to 23	1.2	29 3	103	87 8	163	.92	54	6.32	66	41 5	--
Arietids, southern	Oct. to Nov.	Nov. 5	1.1	27	150	122	6	.85	30	1 91	28	36	2 64
Taurids, northern	Oct. 26 to Nov. 22	Nov. 10	0.4	221	160	308	2 5	86	31	2.16	29	37	3 2
Taurids, night	Nov.		1.0	220	160	300	3	.86	.3	2 1	37	37	3 3
Taurids, southern	Oct. 26 to Nov. 22	Nov 5	0.9	45	157	112	5.1	.85	.36	2 39	28	38	3 69
Leonids[b]	Nov. 15 to 20	Nov. 16 to 17	0 9	234	49	179	162	.92	.99	12 8	72	41	33.25
Bielids[b]	Nov 15 to Dec 6		2 5	250	109	223	13	.76	.88	3.6	16	39.5	6.6
Geminids	Nov. 25 to Dec. 17	Dec. 12 to 13	4 0	261	--	324	24	.90	14	1 4	35	35	1.7
Ursids	Dec. 20 to 24	Dec. 22	2.5	270	--	210	5±3	1 0	.92	--	37	42	--

[a]F = ratio of maximum accumulative meteoroid stream flux to the sporadic meteoroid flux for mass size $\geq 10^{-2}$ grams

[b]Periodic streams

The contribution of each stream to the accumulative meteor stream flux for a calendar year is schematically illustrated in figure 4. For simplification, the flux is considered constant for the entire period of stream activity. This sketch illustrates the inability to have a preferential orientation because of simultaneous occurrence of more than one stream.

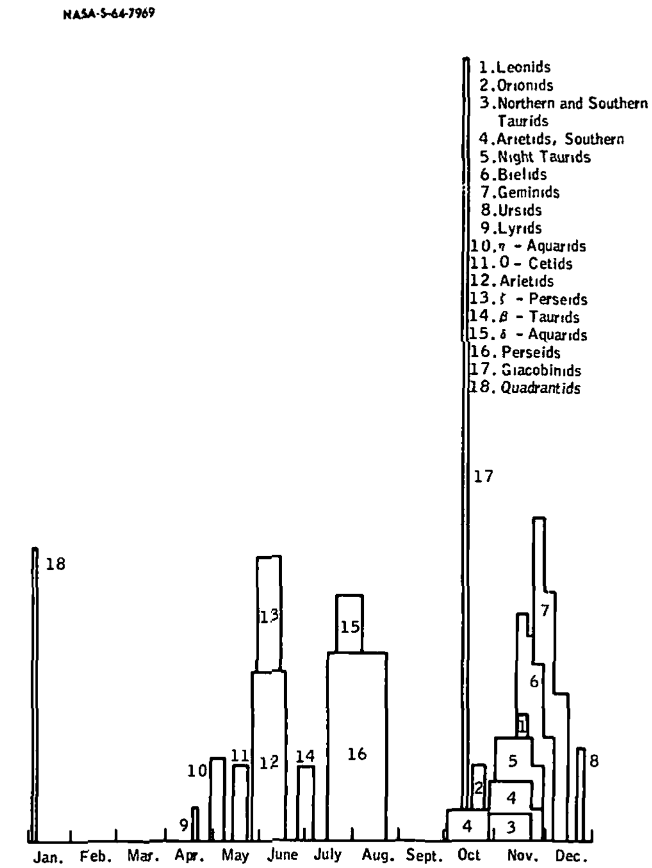

Figure 4. - Accumulative meteoroid stream flux for a calendar year.

Measurements of flux and the variation of flux with magnitude have been made in the visual magnitude range 0 to 3 and in the radar magnitude range 5 to 7 for a number of streams. There is a direct correlation between visual and radar magnitude; hence, the radar measurements are applicable to the visual magnitude scale. The data obtained in the ranges quoted indicate that the flux-visual magnitude slope approaches zero at the fainter visual magnitudes. If the curve of flux as a function of visual magnitude is continuous and the slope does not change sign, the flux at the fainter magnitudes will be less. The fluxes of three streams are presented in figure 5. The slopes of the variation of flux with visual magnitude of Perseids and Geminids decrease (approach zero) with decreasing mass; however, the slope of the Arietids increases for radar magnitudes greater than 2. Measurements of other streams also indicate a trend of decreasing slope of flux as a function of visual magnitude.

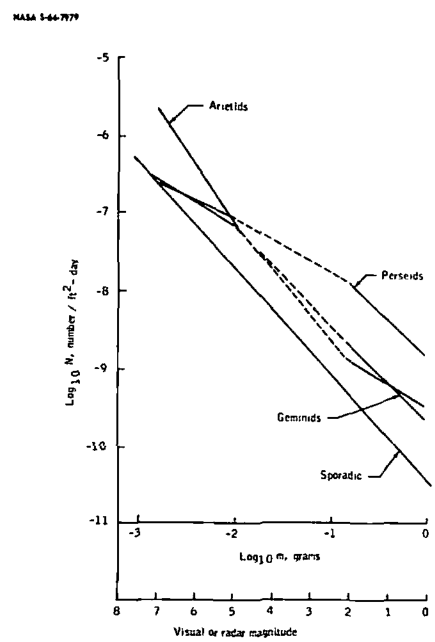

Figure 5. - Variation of meteoroid shower flux.

Only one stream, the Geminids, has been measured at a radar (and visual) magnitude of 8 (corresponding to a mass of 6.31×10^{-4} gm) to determine the variation of flux with time. The results, presented in figure 6, show a marked decrease of F with decreasing mass. Therefore, it seems realistic that a variation of F with mass should be included in the model environment.

NASA-S-64-7980

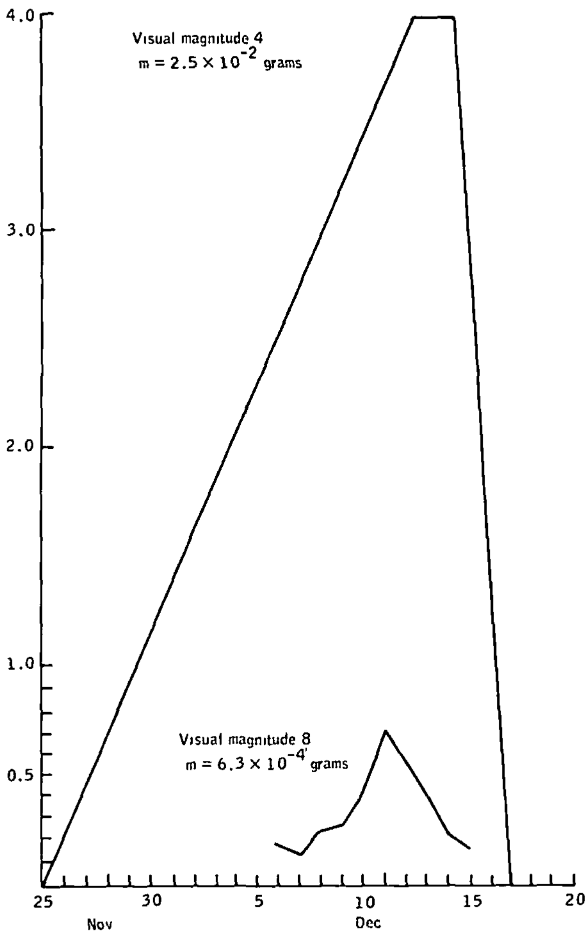

Figure 6 - Comparison of F ratio at visual magnitudes 4 and 8 for Geminid stream

The Quadrantids, Giacobinids, Leonids, and Bielids are periodic streams. The nucleus of the Quadrantids has a predicted period of 13 years; however, measurements indicate an almost random (with respect to years) occurrence of high meteor flux rates associated with the nucleus. The Giacobinids have a well-defined nucleus with a period of 6.5 years, with negligible activity for intervening years. The 6.5-year period will cause a meteoroid influx every 6 or 7 years. On the 13-year period (1933) very heavy meteoroid influxes have been measured (1933 and 1946); however, the peak meteor flux increases over the sporadic background to 15 percent of the maximum meteor rate in $1\frac{3}{4}$ hours. In the next $1\frac{1}{2}$ hours, the flux increases to a maximum and then reduces to 15 percent of maximum. The stream reduces to the sporadic background in another $1\frac{1}{4}$ hours giving a total stream lifetime of $4\frac{1}{2}$ hours.

The Leonid stream has a period of 33.25 years, the intervening years having very low flux rates of approximately 10 meteors per hour. The periodic influx of this stream can only be inferred from past observations. From 1831 to 1833, there was considerable shower activity culminating in an estimated rate of 10 000 meteors/hour in 1833. In 1866, a maximum of 5000 meteors/hour was noted, decreasing to 1000 meteors/hour in 1867 and 1868. In 1901 and 1903, there were 200 to 250 meteors/hour. From 1930 to 1932, the activity increased from 30 to 240 meteors/hour. The

decrease in activity of this stream may be due to perturbations of the stream by the planets or the lack of synchronization of the $33\frac{1}{4}$-year period with the earth's orbit. The 1965 to 1968 period will be 100 years from the time of the last estimated rate of 5000 to 1000 meteors/hour and would put the earth-moon system in close proximity to the nucleus if the orbit has not been disturbed.

The Bielids have indicated an almost constant yearly rate of 20 to 30 meteors/hour. The periodicity of the Bielids is 6.6 years. This would result in many observations of meteor showers associated with the stream nucleus. The constancy of the meteor rates from year to year indicates that the stream has been perturbed and may be regarded as a constant stream.

Secondary Meteoroids

It has been postulated that the impact of primary meteoroids onto the lunar surface will eject material that will, in the rarefied lunar atmosphere, create a secondary flux. Laboratory experiments of hypervelocity impacts into basalt and weakly bonded sand (ref. 14) indicate the secondary flux is approximately 10^4 greater than the primary flux. Additional experiments by Gault and Heitowit of the NASA Ames Research Center involving hypervelocity impacts into dendritic structures of bonded sands, fairy castles, and pumice indicate secondary ejecta exists for all surface structures. The ejecta is 10^3 times the primary flux for a sand having 70 percent porosity and is only significantly reduced (40 times the primary) for the pumice.

MODEL METEOROID ENVIRONMENT

Average Primary Sporadic Meteoroid Flux

The meteoroid environment for near earth, cislunar, and lunar operations is a slightly modified form of the environment submitted in reference 8 to take into consideration new data and to simplify the application to vehicle design. The unshielded meteoroid flux is a modification of the flux-mass relation, presented for an average velocity of 30 km/sec by Whipple as follows:

$$\log N = -1.34 \log_{10} m + 2.68 \log_{10} (0.44/\rho) - 14.48$$

where:

N cumulative number of particles/sq meter-sec of mass, m, and larger

m mass, grams

This equation has been modified to exclude earth shielding, increase the density to 0.5 gm/cm^3 (the trend of the actual density variation was previously discussed), and give N in particles/ft^2-day:

$$\log_{10} N = -1.34 \log_{10} m - 10.423$$

The increase in density gives a slight conservatism in the predicted number of particles for a given mass. It has been postulated in reference 15, but not generally accepted nor proven in the measurements of reference 16, that for particles less than 10^{-8} gm the particle concentration decreases with distance from the earth's surface at a rate inversely proportional to the distance to the 1.4 power, to a minimum value at 10^5 km. This decrease has not been applied to the meteoroid environment. The flux-mass relation is illustrated in figure 7. The minimum particle size cutoff corresponds to a 0.5-gm/cm^3 density with a particle diameter of 4.1 microns and to a 7-gm/cm^3 density with a particle diameter of 0.16 micron. The aforementioned flux-mass relation defines the primary sporadic meteoroid flux for near-earth, cislunar, and lunar operations. The use of this equation states a mass of 1 gm for a visual magnitude of zero, and a visual magnitude-mass relation as follows:

NASA-S-64-7972

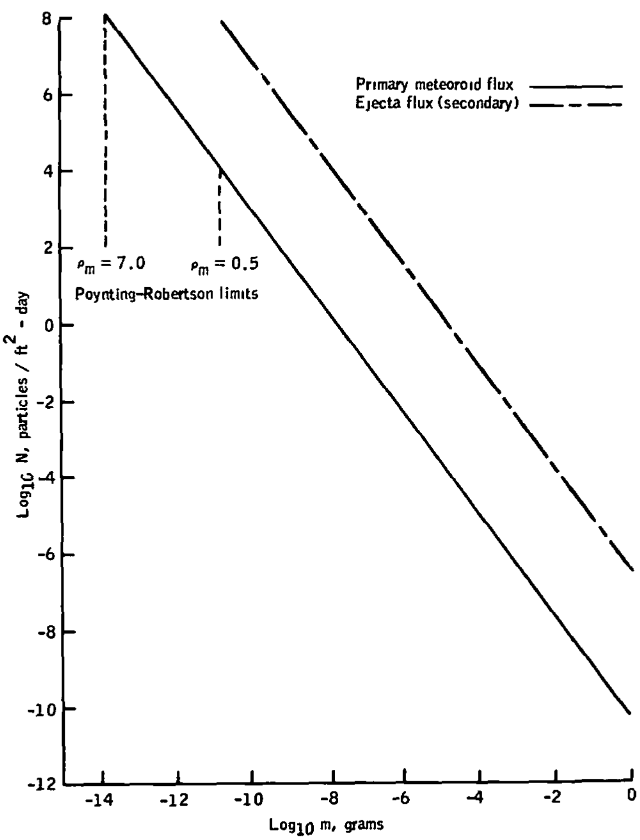

Figure 7. - Earth, cislunar, and near-lunar meteoroid environment.

$$m_n = m_o \, 10^{-0.4 \, M_{v,n}}$$

where:

$M_{v,n}$ n^{th} visual magnitude

m_n mass at M_v of n

m_o mass at M_v of o

The prescribed flux is a yearly average and does not include the month-to-month variation illustrated in figure 8 that has been measured for visual magnitudes equal to and less than 5.

Meteoroid Stream Flux

The rate of meteor influx varies with time for each stream; however, the variation is not well defined. For this model environment, the variation in the rate of meteor influx with time for a stream is represented by a triangle or trapezoid (with the maximum rate of meteors per hour corresponding to the maximum value of the triangle or trapezoid). A triangle represents a stream having a maximum period of activity of 1 day or less; a stream with maximum activity longer than 1 day is represented by a trapezoid. The base of the triangle (the sporadic meteoroid background) corresponds to the total time of stream activity. A straight line variation from sporadic to maximum stream flux is assumed for the beginning and ending of each shower.

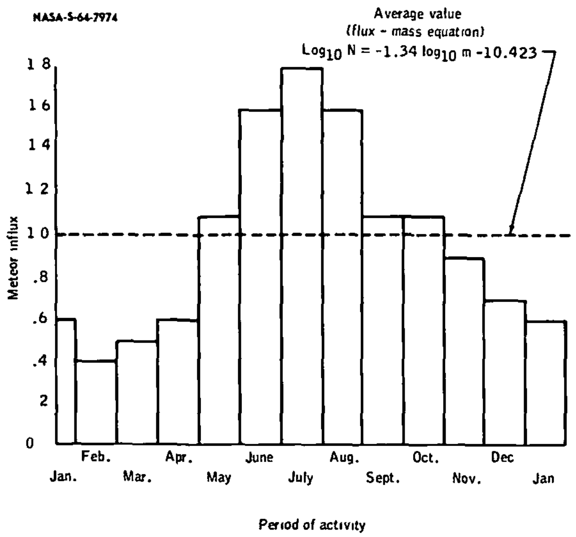

Figure 8. - Yearly sporadic meteor influx.

The F variation for each of the 18 major streams is illustrated in figure 9, and the integrated stream meteor flux for a calendar year is presented in figure 10.

It should be noted that figures 9 and 10 apply only for a visual magnitude of 5 and brighter (that is, a mass of 10^{-2} grams and larger) and extrapolation of this integrated magnification factor to the smaller particle sizes (fainter visual magnitudes) is not valid. The variation of reduced F with time for the smaller masses is illustrated in figure 11. The maximum flux is considered unity for each stream and the duration of the stream is assumed to be the same as that of figure 9. It should be emphasized that these reductions are an interim measure dictated by the current lack of detailed knowledge of streams. The resultant integral of F as a function of time is depicted in figure 12. For meteoroids with masses $\geq 10^{-2}$ gm, the F factors are defined in figures 9 and 10; for masses $< 10^{-2}$ gm, the F factors are defined in figures 11 and 12.

The Quadrantids, Giacobinids, Leonids, and Bielids are periodic streams and are exceptions to the normal meteoroid streams depicted in figure 10. The 13 measured peak flux rates of the Quadrantids from 1864 to 1953 vary from 34 to 180 meteors/hour indicating an ill-defined nucleus. The environment uses an arithmetic average of the measured maximums; that is, 80 meteors/hour, for masses $\geq 10^{-2}$ gm as illustrated in figure 9.

Except for the nucleus, there is no significant meteor activity for Giacobinids. The $6\frac{1}{2}$-year-period maximum F, as shown in figure 10, is 20 for

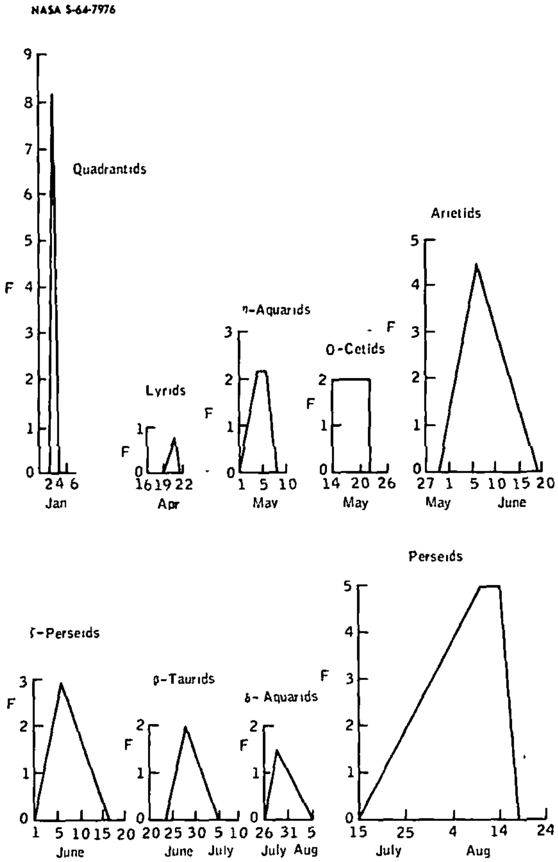

(a) January to August

Figure 9. - Variation of F ratio with date of activity of major meteoroid streams for mass size $\geq 10^{-2}$ grams.

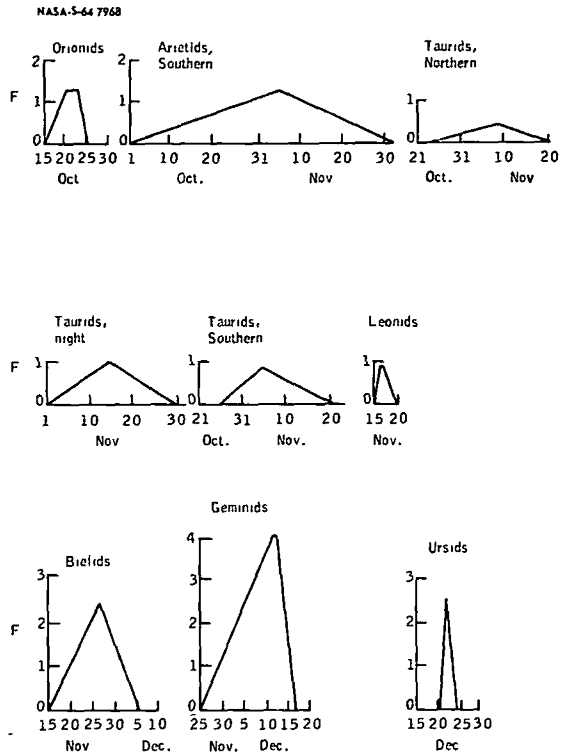

(b) October to December

Figure 9 - Concluded

the Giacobinid nucleus. The 13-year peak has been estimated to be 4000 to 6000 meteors/hour that might next occur in 1972.

There is only the minor activity, illustrated in figure 9, for the portion of the Leonid stream outside the nucleus. The Leonid meteoroid environment has an F value of 25 based on the last two measurements having a 33-year period. Some relief to the stream intensity is obtained by the short-time duration of the stream. The rate of meteors per hour increases from 10 percent of maximum to the maximum in 5 hours and decreases to 50 percent of maximum in another $1\frac{1}{2}$ hours.

As a result of the paucity of information on flux-mass relationships for the individual streams, the stream flux-mass relation is assumed to be the same as the law established for the sporadic activity. Thus, with the use of the ratios from figures 9 and 11, the stream flux-mass relation may be obtained for

NASA-S-64-7970

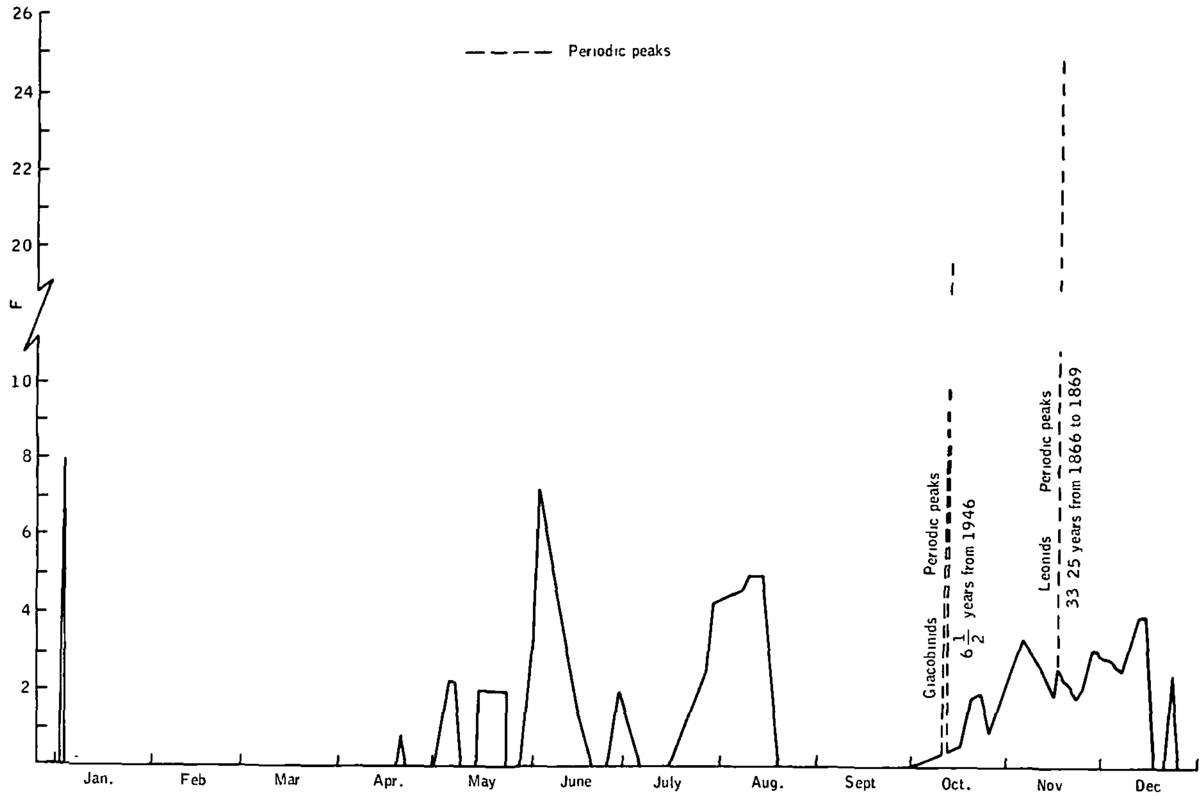

Figure 10.- Ratio of accumulative meteoroid stream flux to the sporadic meteoroid flux for $m \geq 10^{-2}$ grams.

any desired period of stream activity, that is,

$$\log_{10} N_{stream} = -1.34 \log_{10} m - 2.68 \log_{10} V_s - 6.465 + \log_{10} F$$

where:

V_s geocentric velocity of the meteoroid stream, km/sec

F ratio of accumulative meteoroid stream flux to the sporadic meteoroid flux

N number of particles/ft^2-day

This equation takes into consideration the variation of mass with velocity as predicted in reference 17. The mass density of individual stream meteoroids is the same as for the sporadics, assumed to be of cometary origin, which is 0.5 gm/cm^3.

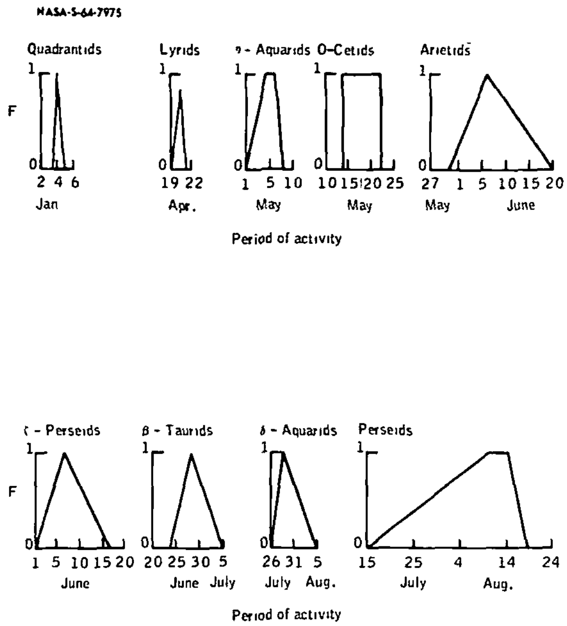

(a) January to August.

Figure 11. - Variation of revised F with date of activity of major meteoroid streams of mass size < 10^{-2} grams

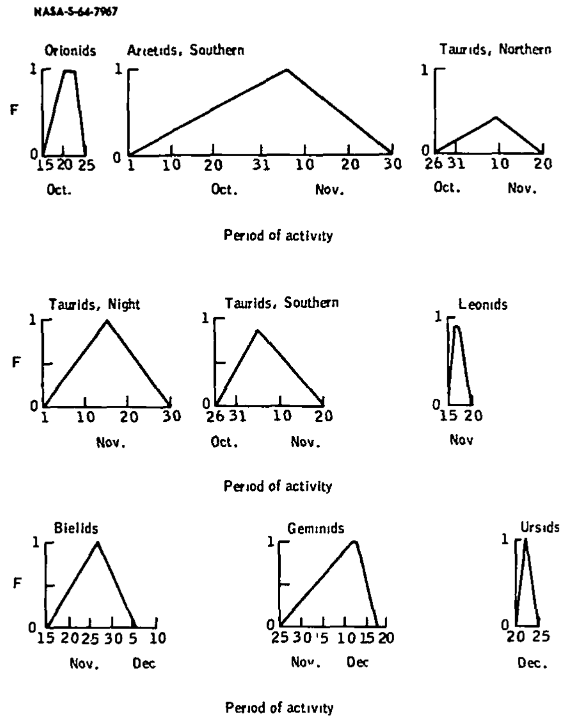

(b) October to December

Figure 11. - Concluded.

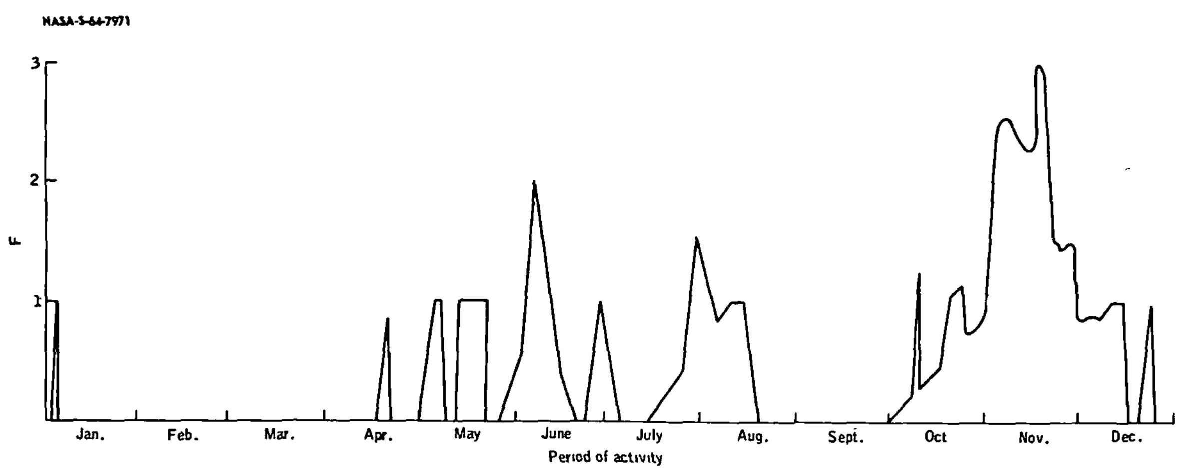

Figure 12. - Ratio of accumulative meteoroid stream flux to the sporadic meteoroid flux for $m < 10^{-2}$ grams in a calendar year.

The total number of impacts or penetrations for a spacecraft exposed to the meteoroid environment is the sum of the sporadic and stream contributions. For the sporadics, the omnidirectional flux dictates the use of total exposed surface area. In the case of the streams, the projected area is used, and the period of stream activity may be obtained from table I or the abscissa of figure 9.

Secondary Flux for the Vicinity of the Moon

The lunar-surface meteoroid flux has a primary component that is composed of the sporadic near earth meteoroid flux, with or without the stream meteoroid flux, and a secondary flux component that is composed of ejecta as a result of primary impingement. The flux of secondary particles, based upon reference 14, is $10^{3.83}$ of the primary and persists to a lunar altitude of 30 kilometers. As a simplification, the ill-defined variation of flux with altitude as presented in reference 14 is not incorporated in this model environment. The density of the ejecta is 2.5 gm/cm^3, with a maximum velocity of 2.4 km/sec. Assuming that 55 percent of the primary particle kinetic energy is distributed in the ejecta particles (ref. 18), the average ejecta velocity is 200 meters/sec. The secondary flux presented in figure 7 includes a shielding factor of one-half, but does not take into consideration the percentage of the ejecta flux that have negligible velocities, nor the effect of streams.

The ejecta flux-mass relation for a sporadic primary can be expressed in particles/ft^2-day as:

$$\log_{10} N_{ejecta} = -1.34 \log_{10} m - 6.59$$

and for a stream primary, in particles/ft^2-day, as:

$$\log_{10} N_{ejecta} = -1.34 \log_{10} m - 2.68 \log_{10} V_s - 2.635 + \log_{10} F$$

In the general case (ejecta from sporadic and stream):

$$N_{ejecta} = 10^{3.83} \times N_{sporadic} + 10^{3.83} \times N_{stream}$$

Shielding Factor

The position of a spacecraft in relation to a shielding body will reduce the exposed area and consequently the number of impacts. The shielding factor ζ for an omnidirectional flux is defined as follows:

$$\zeta = \frac{1 + \cos \theta}{2}$$

where:

$$\sin\theta = \frac{R}{R + H}$$

R radius of shielding body

H altitude above the surface of the shielding body

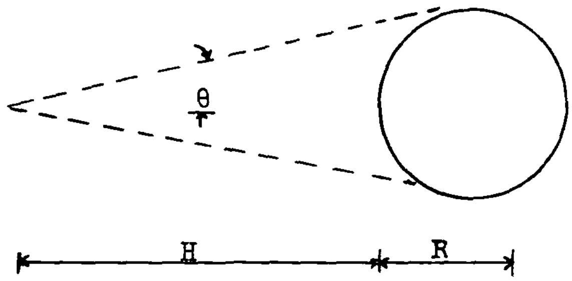

Sketch A

PROJECTED MODIFICATIONS OF THE MODEL METEOROID ENVIRONMENT

The continued research in meteoroid technology will cause modifications to the model meteoroid environment as presented in this paper. Based upon known uncertainties and the areas under investigation, the following revisions are to be expected:

For sporadic meteoroids,

(1) The slope of log flux as a function of log mass of meteoroids will not be constant throughout the mass range.

(2) The density will vary for various mass ranges, at least for the smaller masses.

(3) The average velocity will be replaced by a velocity dependent upon particle mass.

For stream meteoroids,

(1) The flux as a function of mass and time during intercept with the earth's orbit will be determined for the major streams.

(2) The flux variation in portions of the orbits will be defined.

(3) Density of particles in streams may be predicted.

For secondary flux,

(1) A flux-mass distribution will be defined by in situ measurements.

(2) The ejecta will be defined in terms of kinetic energy as a function of particle size.

(3) The distribution of velocity of the ejected mass will be defined.

CONCLUDING REMARKS

The near-earth and cislunar meteoroid environment is composed of a primary meteoroid flux of sporadic and stream meteoroids. The model flux-mass relation for the sporadic population, in particles/ft^2-day, is as follows:

$$\log_{10} N = -1.34 \log_{10} m - 10.423$$

where:

N number of particles/ft^2-day

m mass, grams

The model meteoroid density is 0.5 gm/cm^3 for all particle sizes. The velocity of the sporadic meteoroids is assumed constant for all particle sizes at 30 km/sec.

The flux-mass relationship, applicable to periods of stream activity during the course of a calendar year, in particles/ft^2-day, is defined as follows:

$$\log_{10} N_{stream} = -1.34 \log_{10} m - 2.68 \log_{10} V_s - 6.465 + \log_{10} F$$

where:

F ratio of the stream to sporadic hourly rates

V_s geocentric velocity of an individual stream

The mass density for all shower meteoroids is 0.5 gm/cm^3. The effects of streams on spacecraft may be based on the projected area.

The lunar environment (within 30 km of the lunar surface) is composed of the primary sporadic and stream meteoroid flux plus a secondary flux. The secondary flux N_{ejecta} is defined as follows in particles/ft^2-day:

(1) Sporadic:

$$\log_{10} N_{ejecta} = -1.34 \log_{10} m - 6.59$$

(2) Streams:

$$\log_{10} N_{ejecta} = -1.34 \log_{10} m - 2.68 \log_{10} V_s - 2.635 + \log_{10} F$$

The ejecta density is 2.5 gm/cm^3, and the average velocity is considered to be 200 meters/sec.

A planetary shielding factor is to be used in conjunction with the sporadic population in the vicinity of the earth and the moon. The shielding factor ζ is defined as follows:

$$\zeta = \frac{1 + \cos \theta}{2}$$

where:

$$\sin \theta = \frac{R}{R + H}$$

R radius of shielding body

H altitude above the surface of the shielding body

Manned Spacecraft Center
National Aeronautics and Space Administration
Houston, Texas, December 22, 1964

REFERENCES

1. Berman, Arthur I.: The Physical Principles of Astronautics. John Wiley and Sons, Inc., New York, 1961.

2. Whipple, Fred L.: A Comet Model III, The Zodiacal Light. The Astrophysical Journal, vol. 121, no. 3, 1955, pp. 750-770.

3. Giese, R. H.: Light Scattering by Small Particles and Models of Interplanetary Matter Derived From the Zodiacal Light. Space Sci. Rev., vol. 1, 1962-1963, pp. 589-611.

4. Soberman, R. K.; Hemenway, C. L.; et al.: Micrometeorite Collection From a Recoverable Sounding Rocket. Air Force Cambridge Research Laboratory 1049, Nov. 1961.

5. Harrison, Brown: The Density and Mass Distribution of Meteoritic Bodies in the Neighborhood of the Earth's Orbit. Journal of Geophysical Research, vol. 65, no. 6, June 1960, pp. 1679-1683.

6. Jacchia, Luigi G.; and Whipple, Fred L.: Precision Orbits of 413 Photographic Meteors. Smithsonian Contribution to Astrophysics, vol. 4, no. 4, Smithsonian Institution, Washington, D.C., 1961.

7. Davidson, John R.; and Sandorff, Paul E.: Environmental Problems of Space Flight Structures II. Meteoroid Hazard. NASA TN D-1493, 1963.

8. Whipple, Fred L.: On Meteoroids and Penetration. Journal of Geophysical Research, vol. 68, no. 17, Sept. 1963, pp. 4929-4939.

9. Struve, Otto: Visual Observations of Meteors. Sky and Telescope, vol. 19, no. 4, Feb. 1960, pp. 200-204.

10. Whipple, Fred L.: The Meteoritic Risk to Space Vehicles. Proc. of the VIIIth International Astronautical Cong. Springer-Verlag (Vienna), 1958, pp. 418-428.

11. Lovell, Alfred C. B.: Meteor Astronomy. Oxford University Press, London, 1954.

12. Kallman, H. K.: Relationship Between Masses and Visual Magnitudes of Meteors. Meteors. (Special Supplement (vol. II) to the Journal of Atmospheric and Terrestrial Physics). T. R. Kaiser, ed., Pergamon Press,, 1955, pp. 43-54.

13. Middlehurst, Barbara M.; and Kuiper, G. P.: The Moon, Meteorites and Comets. The Solar System, vol. IV. Chicago University Press, 1963.

14. Gault, Donald E.; Shoemaker, Eugene M.; and Moore, Henry J.; Spray Ejected From the Lunar Surface, NASA TN D-1767, 1963.

15. Whipple, Fred L.: The Dust Cloud Around the Earth. Nature, vol. 169, Jan. 1961, p. 127.

16. Alexander, W. M.; McCracken, C. W.; Secretan, L.; and Berg, O. E.: Review of Direct Measurements of Interplanetary Dust From Satellites and Probes. Presented at the Committee on Space Research Meeting, May 1962 (NASA TM X-613-62-25).

17. Opik, Ernst J.: Physics of Meteor Flight in the Atmosphere. Interscience Tracts on Physics and Astronomy, no. 6, Interscience Publishers, New York, 1958.

18. Gault, D. E.; and Heitowit, E. Z.: The Partition of Energy for Hypervelocity Impact Craters Formed in Rock. Proceedings of the Sixth Symposium on Hypervelocity Impact, vol. II, part 2, The Firestone Tire and Rubber Co., Cleveland, Ohio, Aug. 1963.

"The aeronautical and space activities of the United States shall be conducted so as to contribute . . . to the expansion of human knowledge of phenomena in the atmosphere and space. The Administration shall provide for the widest practicable and appropriate dissemination of information concerning its activities and the results thereof."

—NATIONAL AERONAUTICS AND SPACE ACT OF 1958

NASA SCIENTIFIC AND TECHNICAL PUBLICATIONS

TECHNICAL REPORTS: Scientific and technical information considered important, complete, and a lasting contribution to existing knowledge.

TECHNICAL NOTES: Information less broad in scope but nevertheless of importance as a contribution to existing knowledge.

TECHNICAL MEMORANDUMS: Information receiving limited distribution because of preliminary data, security classification, or other reasons.

CONTRACTOR REPORTS: Technical information generated in connection with a NASA contract or grant and released under NASA auspices.

TECHNICAL TRANSLATIONS: Information published in a foreign language considered to merit NASA distribution in English.

TECHNICAL REPRINTS: Information derived from NASA activities and initially published in the form of journal articles.

SPECIAL PUBLICATIONS: Information derived from or of value to NASA activities but not necessarily reporting the results of individual NASA-programmed scientific efforts. Publications include conference proceedings, monographs, data compilations, handbooks, sourcebooks, and special bibliographies.

Details on the availability of these publications may be obtained from:

SCIENTIFIC AND TECHNICAL INFORMATION DIVISION

NATIONAL AERONAUTICS AND SPACE ADMINISTRATION

Washington, D.C. 20546